Cluster generalization of the coherent-potential approximation on the basis of projection formalism in augmented space. II. Results of numerical calculations

1991 J. Phys.: Condens. Matter 3 9025

(http://iopscience.iop.org/0953-8984/3/46/004)

J. Phys.: Condens. Matter 3 (1991) 9025–9032. Printed in the UK

Cluster generalization of the coherent-potential approximation on the basis of projection formalism in augmented space: II. Results of numerical calculations

A K Arzhnikov, L V Dobisheva and S G Novokshonov
Physics-Technical Institute, Academy of Sciences of USSR, Ural Branch, 132 Kirov Street, SU-426001 Izhevsk, USSR

Received 25 February 1991

Abstract. The numerical analysis of the equations of the self-consistent approximations of electron self-energy in the binary alloy model with diagonal disorder on a square lattice has been carried out. The calculation of the density of states in the impurity band in the coherent-potential approximation and its generalizations taking into account the fluctuations on the nearest-neighbour pairs and also on the clusters consisting of four nearest neighbours has been performed. The results of the latter reproduce best of all the main peculiarities of the density-of-states histogram obtained by computer simulation on the square lattice containing 100×100 sites.

1. Introduction

This paper is devoted to the numerical analysis of the approximations proposed in the previous paper of this series [1]. The calculation of the density of the single-electron states in a binary alloy model with diagonal disorder on the two-dimensional square lattice with Hamiltonian H and distribution of the random quantities $P_{\xi_i}(\mathscr{E})$ given by

$$H = \sum_i |i\rangle \xi_i \langle i| + \sum_{\langle ij \rangle} |i\rangle V \langle j| \qquad (1)$$
$$P_{\xi_i}(\mathscr{E}) = c\delta(\mathscr{E} - \mathscr{E}_1) + (1-c)\delta(\mathscr{E} - \mathscr{E}_2)$$

is performed; the symbol $\langle ij \rangle$ means summation over all pairs of nearest neighbours. In other respects the notation used here coincides with that adopted in [1]. All calculations are carried out at the following values of the considered model parameters: $\mathscr{E}_1 = -\mathscr{E}_2 = 1.0$, $c = 0.1$, $V = 0.25$. They are in the most interesting range of strong scattering and quite high concentrations. To compare the results, a numerical analysis of the distribution of the eigenvalues of the random operator (1) was made on the two-dimensional square lattice containing 100×100 sites with the boundary condition $V = 0$ at the surface. This analysis was performed for the fixed realization of the Hamiltonian (1) by the method using the theorems on the inertia of congruent matrices [2]. The histogram of the eigenvalue distribution in energy was built by the results. The choice of the two-dimensional model is due to the possibility of a sufficiently reliable comparison of the results of the approximations proposed in [1] with those of numerical

0953-8984/91/469025 + 08 $03.50

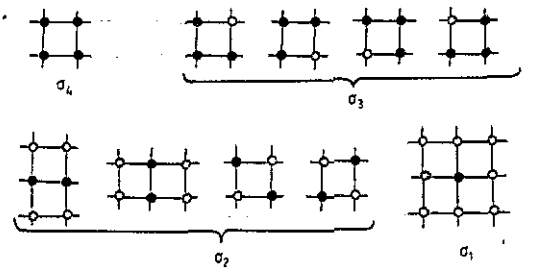

Figure 1. Clusters on which scattering is taken into account (full circles).

simulation on a finite lattice. In fact, in the three-dimensional case the relative weight of the surface (~28 at.%) for a given number of sites ($\sim 10^4$) is high relative to the bulk, which undoubtedly leads to high distortion of the eigenvalue distribution.

When analysing the self-consistent equations for the electron self-energy $\Sigma_0(E, q)$, we limited ourselves to two approximations. In one of them the fluctuations in the nearest-neighbour pairs were taken into account, in the other those in the square cell consisting of four sites σ_4, as well as in all the clusters $\sigma_n \subseteq \sigma_4$. The scattering by the clusters of other configurations is supposed to be negligible. Indeed, the analysis of the corrections to this approximation, similar to that conducted in [1], shows that all of them are small in parameter $\exp(-a/l_0)$, where a is the lattice constant and l_0 is the mean free path of the electron. The exception is the contribution from scattering by the pair of sites at distance $2a$, but we neglect it for simplifying the calculations. The validity of such an approximation was discussed in [1].

2. Self-consistent equations for the self-energy

In this section we discuss the derivation of the self-consistent equations for $\Sigma_0(E, q)$, where the scattering by the clusters $\sigma_n \subseteq \sigma_4$ ($n \leqslant 4$) depicted in figure 1 by the full circles is taken into account. To this end, according to the self-consistency procedure proposed in [1], let σ_4 be the only maximum cluster in this case. After this we make the substitution (I.25) in (I.24) (see [1]) at all levels up to the fourth for those i, j which satisfy at least one of the conditions: $i \cup \sigma_n \notin \sigma_4$ or $j \cup \sigma_n' \notin \sigma_4$ ($n \leqslant 4$, $\sigma_n \in \sigma_4$, $\sigma_n' \in \sigma_4$). As a result we obtain the expression for the self-energy

$$\Sigma_0(E, q) = \Delta_0(q) \frac{1}{E - \mathcal{H}_1^{\text{eff}}(E) - W_1(E) - \tilde{\Sigma}_1(E, q)} \Delta_0^+(q)$$
$$\tilde{\Sigma}_n(E, q) = \tilde{\Delta}_n(q) \frac{1}{E - \mathcal{H}_{n+1}^{\text{eff}}(E) - W_{n+1}(E) - \tilde{\Sigma}_{n+1}(E, q)} \tilde{\Delta}_n^+(q). \tag{2}$$

Here

$$\tilde{\Delta}_n(q) = \sum_{\substack{\sigma_n, i \notin \sigma_n \\ i \cup \sigma_n = \sigma_{n+1} \in \sigma_4}} |i, \sigma_n, q) \xi' \exp(-iqd) (i - d, \sigma_{n+1}, q|$$

$$W_n(E) = \sum_{\sigma_n, i \in \sigma_n} |i, \sigma_n, q) (\hat{\xi} - \bar{\xi}) (i, \sigma_n, q| - \sum_{(1)} |i, \sigma_n, q) \Sigma_{ij}^{\text{eff}}(E)$$
$$\times (j, \sigma_n, q| - \sum_{(2)} |i, \sigma_n, q) \Sigma_{ij}^{\text{eff}}(E) (j, \sigma_n, q| \tag{3}$$

where $\Sigma_{(1)}$ means summation over σ_n and i, j, such that at least one of them satisfies the

condition $i \in \sigma_n$ or $j \in \sigma_n$; $\Sigma_{(2)}$ means summation over σ_n and i, j, satisfying the conditions $i \notin \sigma_n, i \cup \sigma_n \subseteq \sigma_4$ and $j \notin \sigma_n, j \cup \sigma_n \subseteq \sigma_4$ simultaneously. In figure 1 the sites satisfying the last conditions are marked by open circles. In other respects the notation adopted here coincides with that used in [1].

For further consideration the matrices of operators $G_n^{\mathrm{eff}}(E)$ and $W_n(E)$ are convenient to represent in block form by the appropriate rearrangement of the rows and lines

$$\begin{pmatrix} G_n^{\mathrm{eff}(1)} & \tilde{G}_n^{\mathrm{eff}(3)} \\ G_n^{\mathrm{eff}(3)} & G_n^{\mathrm{eff}(2)} \end{pmatrix} \qquad \begin{pmatrix} W_n^{(1)} & \tilde{W}_n^{(3)} \\ W_n^{(3)} & 0 \end{pmatrix} \tag{4}$$

where $[A_n^{(1)}]_{ij}$, $i \cup \sigma_n \in \sigma_4$, $j \cup \sigma_n \in \sigma_4$; $[A_n^{(3)}]_{ij}$, $i \cup \sigma_n \notin \sigma_4$, $j \cup \sigma_n \in \sigma_4$; $[A_n^{(2)}]_{ij}$, $i \cup \sigma_n \notin \sigma_4$, $j \cup \sigma_n \notin \sigma_4$. This representation allows us to perform in (2) all necessary inversions of the matrices. In fact, owing to the restrictions imposed on i, j in the operators $\tilde{\Delta}_n(q)$ (3), we have to calculate the inverted matrices on the right-hand sides of (2) not entirely, but only one block of the type $A_n^{(1)}$ of each matrix. It can be done using the Frobenius formulae of matrix inversion in block form. After these transformations the problem of the calculation of $\Sigma_0(E, q)$ reduces to the determination of a single element of the inverse matrix of the following:

$$D = \begin{pmatrix} A_1 & \tilde{B}_1 & & & & & \\ B_1 & C_1 & S_1 & & & & \\ & S_1^+ & A_2 & \tilde{B}_2 & & & \\ & & B_2 & C_2 & S_2 & & \\ & & & S_2^+ & A_3 & \tilde{B}_3 & \\ & & & & B_3 & C_3 & S_3 \\ & & & & & S_3^+ & A_4 \end{pmatrix} \tag{5}$$

$$\Sigma_0(E, q) = (\xi')^2 [D^{-1}]_{11}.$$

Here S_n is a diagonal matrix consisting of the matrix elements $\xi' \exp(-iqd)$ of the operator $\tilde{\Delta}_n(q)$ (3),

$$\begin{pmatrix} A_n & \tilde{B}_n \\ B_n & C_n \end{pmatrix} = \Gamma_n^{-1} - W_n^{(1)} - \tilde{W}_n^{(3)} G_n^{\mathrm{eff}(2)} W_n^{(3)}$$
$$\Gamma_n^{-1} = (1 - \tilde{W}_n^{(3)} G_n^{\mathrm{eff}(3)})(G_n^{\mathrm{eff}(1)})^{-1}(1 - \tilde{G}_n^{\mathrm{eff}(3)} W_n^{(3)}). \tag{6}$$

The convolutions in these expressions can be presented through the products of the corresponding matrices of finite dimensions and the Fourier integrals

$$\Sigma_{ij}^{\mathrm{eff}}(E) = \frac{1}{(2\pi)^2} \iint \Sigma_q^{\mathrm{eff}}(E) \exp[iq(i-j)]\, \mathrm{d}^2 q$$

$$G_{ij}^{\mathrm{eff}}(E) = \frac{1}{(2\pi)^2} \iint G_q^{\mathrm{eff}}(E) \exp[iq(i-j)]\, \mathrm{d}^2 q$$

$$I_{ij}^{(1)}(E) = \frac{1}{(2\pi)^2} \iint G_q^{\mathrm{eff}}(E) \Sigma_q^{\mathrm{eff}}(E) \exp[iq(i-j)]\, \mathrm{d}^2 q \tag{7}$$

$$I_{ij}^{(2)}(E) = \frac{1}{(2\pi)^2} \iint G_q^{\mathrm{eff}}(E) [\Sigma_q^{\mathrm{eff}}(E)]^2 \exp[iq(i-j)]\, \mathrm{d}^2 q$$

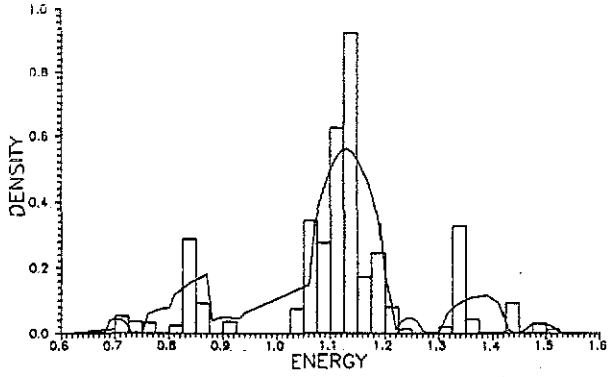

Figure 2. Density of states in the impurity band, obtained in the self-consistent approximation with due account of fluctuations at $\sigma_n \subseteq \sigma_4$. The histogram of the number of states in the lattice of 100×100 sites ($\mathscr{E}_1 = -\mathscr{E}_2 = 1.0$, $c = 0.1$, $V = 0.25$).

where integration is conducted over the first Brillouin zone of the lattice considered.

The diagonal blocks in (5) are obviously of the following dimension: $A_1\,(1 \times 1)$, $C_1\,(8 \times 8)$, $A_2\,(8 \times 8)$, $C_2\,(12 \times 12)$, $A_3\,(12 \times 12)$, $C_3\,(4 \times 4)$, $A_4\,(4 \times 4)$. Thus the rank of the matrix D (5) is equal to 49. Using the lattice symmetry, some of the matrices A_n, B_n and C_n can be diagonalized by unitary transformations and some of the inversions necessary for the calculation of $\Sigma_0(E, q)$ (5) can be performed analytically.

Setting in (5) $\Sigma_0(E, q) = \Sigma_q^{\text{eff}}(E)$ we obtain the system of equations in 14 independent variables. Since integration in (7) can be conducted only numerically, we actually deal with a system of non-linear functional equations.

To conclude this section we note that different approximations for the self-energy, constructed with figured continued fractions, should have the structure analogous to (5) and (6) irrespective of the lattice dimension. The rank of the matrix D (5) will be defined by the number and configuration of the clusters, the scattering by which is taken into account in this approximation. Accordingly the number of independent variables is also defined in the system of equations obtained.

3. Discussion of the numerical analysis results

As stated above, the chosen values of the parameters in (1) correspond to the case of strong scattering. There is a gap between the impurity and host bands, the former being in the energy range (0 to 2), the latter in the range (-2 to 0) [3]. At the concentration of the first component $c = 0.1$ the changes in the host band as compared to the ideal crystal ($c = 0$) are small. So we concentrate all attention upon calculations in the energy range (0 to 2) corresponding to the impurity band.

Figure 2 shows the histogram of the density of states on the lattice containing 100×100 sites and its diagram obtained in the self-consistent approximation taking into account the fluctuations in all clusters $\sigma_n \subseteq \sigma_4$. The count of the number of clusters formed by the impurity atoms in the given configuration (figure 1) may prove that the groups of levels in the histogram near the energies 0.84 and 1.34 coincide with the states bounded at the following pairs of nearest neighbours: 0.74, 1.44—at three atoms; 0.7,

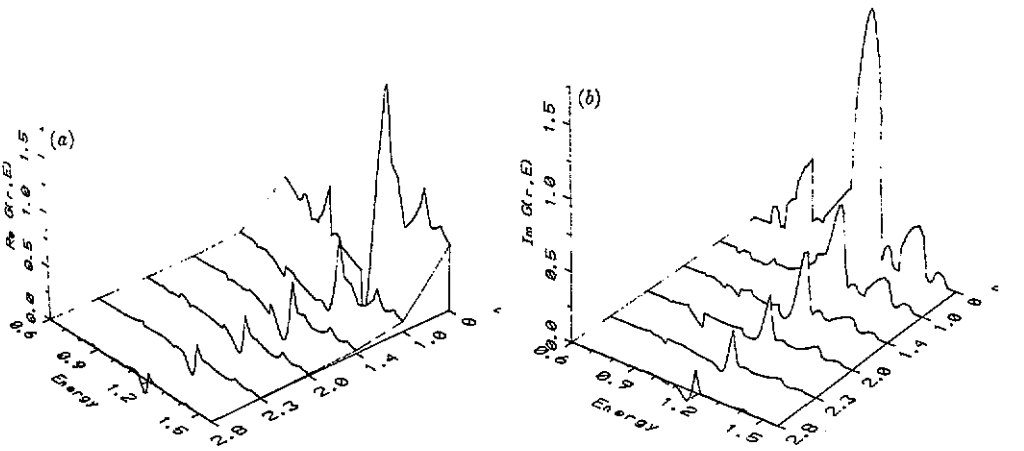

Figure 3. (*a*) Real part and (*b*) imaginary part of the averaged Green function in the self-consistent approximation with allowance for $\sigma_n \subseteq \sigma_4$.

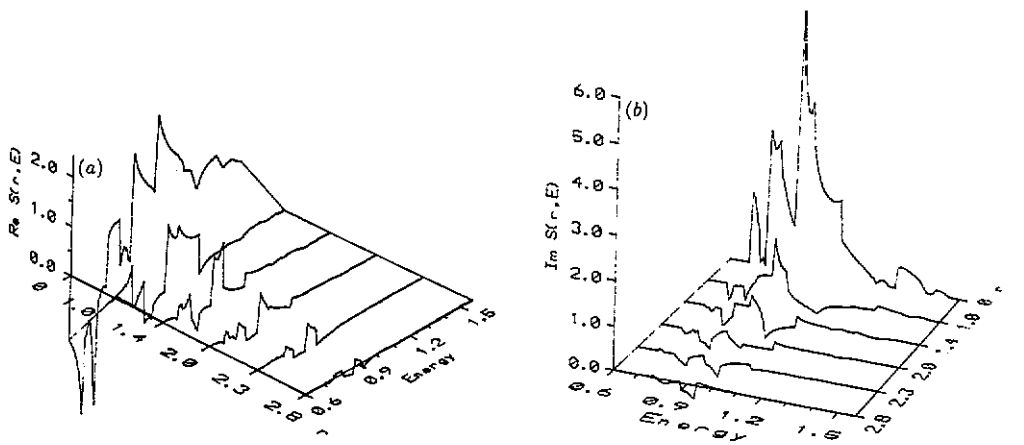

Figure 4. (*a*) Real part and (*b*) imaginary part of the self-energy in the self-consistent approximation with allowance for $\sigma_n \subseteq \sigma_4$.

1.5—at four impurity atoms. As seen from figure 2 the result of the self-consistent calculation has repeated the principal peculiarities of the histogram. The asymmetry of the density-of-states dependence on energy relative to the centre of the band is due to the well known phenomenon of level repulsion [3]. Taking account of the fluctuations in clusters formed by five or more impurity atoms does not appear to change essentially the density-of-states dependence behaviour. Indeed their contribution begins with terms proportional to c^5. The relative changes in the density of states resulting from taking into account the scattering on pairs of fourth, fifth and more remote neighbours i and j should be small due to the smallness of the parameter $G_{ij}^{\text{eff}}(E)/G_{00}^{\text{eff}}(E)$. Only the scattering on third neighbours pairs (the distance between them being equal to $2a$, where a is the lattice constant) can result in visible alterations of the density of states near the

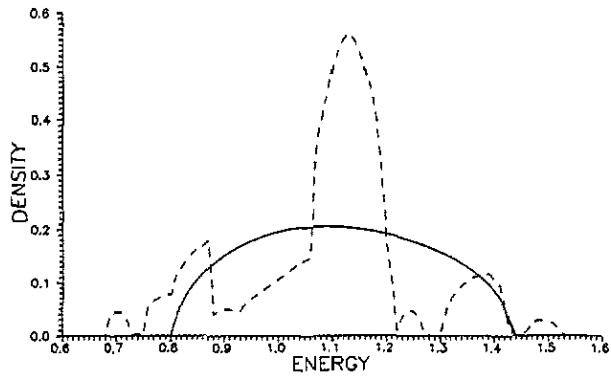

Figure 5. The density of states in the CPA (——) and in the self-consistent approximation with allowance for $\sigma_n \subseteq \sigma_4$ (– – –).

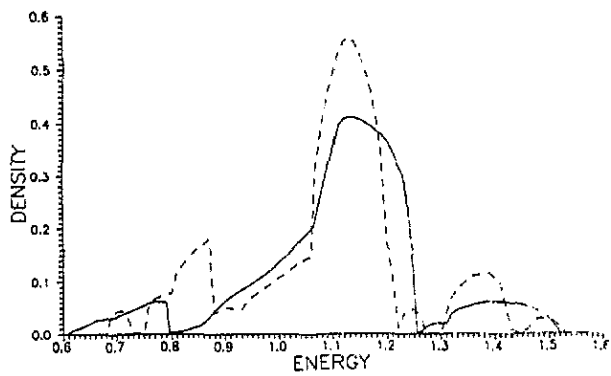

Figure 6. The density of states in the self-consistent approximation with allowance for fluctuations at the nearest-neighbour pairs (analogue of the TCA) (——) and in the self-consistent approximation with allowance for $\sigma_n \subseteq \sigma_4$ (– – –).

impurity band centre. In the histogram their influence becomes apparent in the local maxima near the points 0.96 and 1.2. Thus the considered self-consistent approximation taking account of the scattering on all clusters $\sigma_n \subseteq \sigma_4$ gives a sufficiently good quantitative description of the density of states in the impurity band.

Estimating the errors of different approximations in [1] and in this paper we have used the nature of the dependence of the matrix elements $G_{ij}^{\text{eff}}(E)$ and $\Sigma_{ij}^{\text{eff}}(E)$ on $|i-j|$. In figures 3 and 4 the diagrams of these dependences are shown and it can be seen that indeed $G_{ij}^{\text{eff}}(E)$ and $\Sigma_{ij}^{\text{eff}}(E)$ decrease sufficiently quickly as $|i-j|$ increases.

The results of the density-of-states calculation in the coherent-potential approximation (CPA) and in the self-consistent approximation taking account of the scattering on nearest-neighbour pairs are shown in figures 5 and 6. The latter approximation is an analogue of the travelling-cluster approximation (TCA) [4] in the two-dimensional case. As seen from the comparison of these results with those shown in figure 2, the CPA (figure 5) does not repeat at all the fine structure of the impurity band and only the centre-of-mass position coincides with reality. With the self-consistent account of the scattering

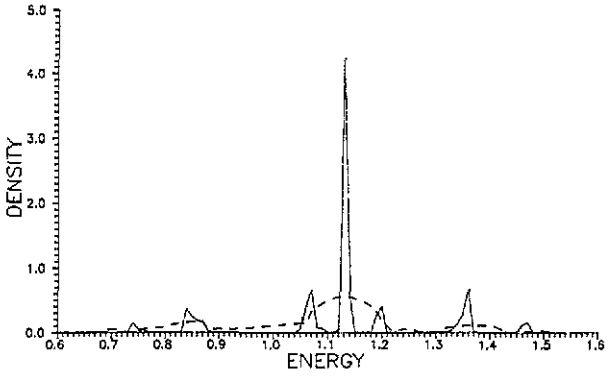

Figure 7. The density of states in the non-self-consistent approximation with allowance for scattering at $\sigma_n \subseteq \sigma_4$ (——) and in the self-consistent approximation (– – –).

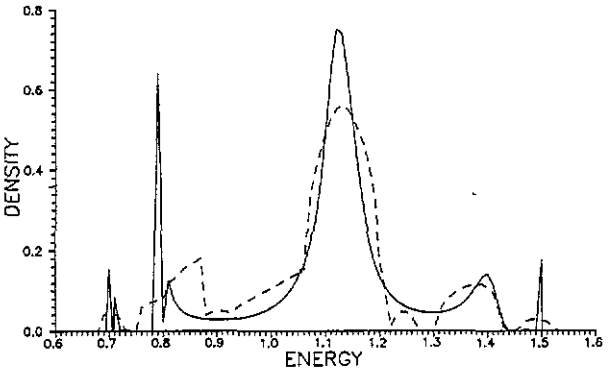

Figure 8. The density of states in the partially consistent approximation (the CPA with non-self-consistent allowance for scattering at $\sigma_n \subseteq \sigma_4$) (——) and in the self-consistent approximation (– – –).

on nearest-neighbour pairs (figure 6), the central region of the impurity band formed by the single-site states is described well enough. At the same time the width of the regions caused by the two-site states is apparently larger.

As was noted before in the self-consistent approximations, the number of independent variables (7) and equations in them increases with increasing number of clusters, the scattering on which is taken into consideration. That leads to increase of computer time for the solution. Besides, during the calculation it was found that, near the maximum of Im $\Sigma^{\text{eff}}(E)$ that is near the states strongly interacting with the host band [3], the simple iteration method ceases to converge, which is in disagreement with one of the conclusions of [4]. That is why it is necessary to use modified methods of solution, for example the Newton method, which also leads to computer time increase. Since this expenditure in more realistic models of alloys may be insuperable, it is of great interest to analyse the non-self-consistent approximations.

Figure 7 shows the calculation result in the non-self-consistent approximation considering the fluctuations in the clusters $\sigma_n \subseteq \sigma_4$. In this approximation the density of

states is a set of sharp peaks. Although their centre positions coincide approximately with the energy levels of the electrons bounded at the nearest-neighbour pair and other clusters belonging to σ_4, this approximation is hardly considered to be successful. More convenient here is the approximation where taking into account the scattering on isolated sites is conducted in a self-consistent way, and at other clusters $\sigma_n \subseteq \sigma_4$ in a non-self-consistent way. This approximation can be obtained by putting into the right-hand side of equation (5) $\Sigma^{\text{eff}}(E)$ calculated in the CPA. Figure 8 shows the density of states obtained in such a way. Here we have better accordance than in figure 7 with the results of both numerical simulation and the self-consistent calculation depicted in figure 2. Because of the dependence of the small parameter m of the theory $(a/R_0)^m$ on the dimensionality, we have grounds to expect that such approximations in the three-dimensional case will be more effective.

References

[1] Arzhnikov A K, Dobisheva L V and Novokshonov S G 1991 *J. Phys.: Condens. Matter* **3** 9015
[2] Parlett B N 1980 *The Symmetric Eigenvalue Problem* (Englewood Cliffs, NJ: Prentice-Hall) p 382
[3] Ehrenreich H and Schwartz L M 1976 *Solid State Physics* vol 31, ed H Ehrenreich, F Seitz and D Turnbull (New York: Academic) p 150
[4] Kaplan T, Leath P L, Gray L J and Diehl H W 1980 *Phys. Rev.* B **21** 4230